Hindawi Publishing Corporation
Journal of Applied Mathematics
Volume 2014, Article ID 801781, 9 pages
http://dx.doi.org/10.1155/2014/801781

Research Article

An Analytical Solution by HAM for Nonlinear Simulation of Deepwater SCR Installation

Yi Wang,[1] Ji-jun Gu,[1] Chen An,[1] Meng-lan Duan,[1] and Ning He[2]

[1] *Offshore Oil/Gas Research Center, China University of Petroleum, Beijing 102249, China*
[2] *Offshore Oil Engineering Co., Ltd., Tianjin 300452, China*

Correspondence should be addressed to Yi Wang; wangyizyn@sina.com

Received 10 December 2013; Revised 29 May 2014; Accepted 5 June 2014; Published 2 July 2014

Academic Editor: Aderemi Oluyinka Adewumi

Steel catenary riser (SCR) is a cost-effective riser system that is widely used in deepwater offshore oilfields development. During SCR J-lay installation, the movement of pull-head must be carefully controlled to ensure riser safety. Since the SCR installation path calculation through numerical simulation software is usually time-consuming, this paper has established a mechanical model for SCR installation by making use of homotopy analysis method (HAM) to simplify its analytical solution, and dimensional analysis was considered in making initial guess solution. Based on this analytical solution, a program within the framework of MATLAB was developed to predict the two-dimensional riser behavior during installation, and a sensitivity analysis for different values of the control variables was carried out. Engineers may efficiently optimize the installation path by the application of this technique.

1. Introduction

In response to increasing global demand of energy from fossil fuels and the replacement of depleting oil and gas reserves in most matured fields in the world, operating companies in the oil industry are expanding their exploration and production operations into deepwater. In deepwater exploration, SCRs are widely used as a cost-effective riser system which is connecting offshore platforms and subsea production systems. During SCR installation as shown in Figure 1, the pull-head is transferred from installation vessel to platform by Abandon & Recovery (A&R) wire from installation vessel and pull-in wire from the platform. The transfer process is usually carried out by J-lay vessel, since the S-lay vessel cannot install SCR independently [1, 2]. The transfer process is divided into prelay and postlay, depending on whether the offshore platform is on site [3].

The shape of SCR will be affected by the route of pull-head during installation controlled by both the A&R and the pull-in wire, and the maximum stresses to be encountered during the transfer process must be obtained before installation [4]. A large number of papers have been published on this issue. The catenary theory is a simple model for evaluating the tension and curvature of SCR [5], but it cannot simulate the rapid change of the inclination angle because it ignores the bending stiffness [6]. The nonlinear large deformation beam theory is more appropriate for simulating the riser near touchdown point (TDP) considering the large-angle deformation [7, 8]. Dixon and Rultledge [9] applied Plunkett's expansions in analyzing J-lay method. Guarracino and Mallardo [10] developed the expansions to analyze the S-lay method. Dai et al. [11] used line integration technique to analyze the tensions of A&R wire while considering the movement of installation vessel. Xing et al. [12] established a nonlinear mechanical model to analyze the pipeline lifting process and applied a shooting method in solving the moving boundary problem. Lenci and Callegari [13] investigated some analytical models to analyze the J-lay method, but the solution is not easy to obtain because the equations are highly nonlinear. García-Palacios et al. [14] used two-dimensional Navier-Bernoulli beam to analyze pipeline laying process, and an updated Lagrangian formulation for the nonlinear analysis was obtained. Nowadays, finite element software such as OrcaFlex is commonly used to solve optimal installation path problem. But it might be time-consuming depending on the performance of computer. Therefore, a simple and

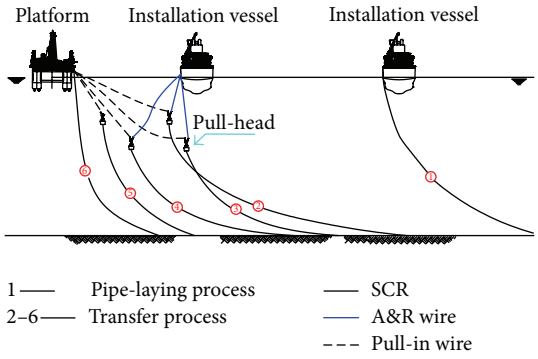

Figure 1: SCR installation procedure.

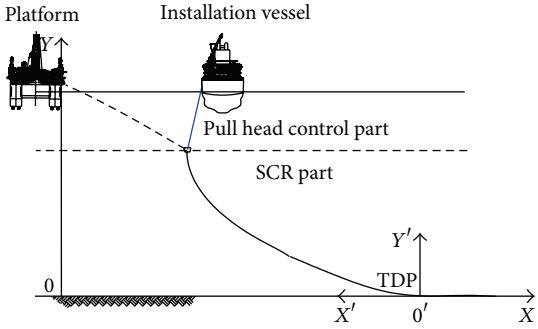

Figure 2: Mechanical model for transfer process of SCR installation.

effective SCR installation model is still important for engineers to understand the nature and relevance of the complex phenomena during installation. Thus, an analytical solution for SCR installation can substantially reduce design time and provide a quick evaluation of actual installation setting.

The structural model presented in this paper is a simple and practical method to obtain the static configuration and the mechanical load parameters for SCR transfer process. The bending stiffness and large deformation of the part suspended in water are taken into consideration. The governing equation system is derived and the analytical approximate solution is obtained by means of HAM. Compared with the available commercial software such as OrcaFlex, the calculation of the present model has the advantage of high stability and being time-saving. A series of parameters such as initial installation angle, maximum lower depth of pull-head, water depth, and distance between installation vessel and offshore platform are considered during the stress analysis of SCR installation.

2. Nonlinear Model of SCR Installation

The mechanical model used to simulate the behavior of transfer process during SCR installation is composed of two parts, as presented in Figure 2. In pull-head control part, the catenary theory is used to simulate the A&R wire and pull-in wire [15]. In SCR part, the nonlinear large deformation beam theory is used to simulate the suspended segment [16]. The hypotheses considered in the model are summarized as follows.

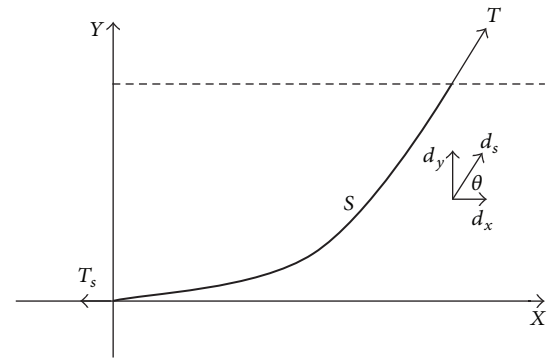

Figure 3: Catenary axis and forces.

(1) The dynamic movement of the installation vessel and platform are not considered.

(2) The gravitational and hydrostatic forces are the only loads upon the riser during installation operations.

(3) The SCR material is linear elastic, and the behavior of SCR is modeled as a two-dimensional beam subjected to axial and bending deformations. Torsional and shear deformation are not considered.

(4) The seabed is rigid. Two parts of the model are solved in the local coordinate system $X'O'Y'$, respectively and transformed to the global coordinate system XOY, finally. The TDP of SCR is the origin of local coordinate system $X'O'Y'$.

2.1. Pull-Head Control Part. The location of pull-head is important for SCR shape control. It is controlled by the length of A&R wire from installation vessel and pull-in wire from platform. Based on catenary theory as shown in Figure 3, the following equations can be obtained:

$$S = \sqrt{y^2 + 2\frac{T_s}{w}y} \tag{1}$$

$$x = \frac{T_S}{w}\ln\left[\frac{w}{T_S}y + 1 + \sqrt{\left(\frac{w}{T_S}y + 1\right)^2 - 1}\right], \tag{2}$$

where T is axial tension at pull-head, T_s is axial tension at TDP, w is the submerged weight per unit length of the riser, and S is the length of SCR.

The transfer process is typically carried out by two steps. The first step is to lower the pull-head by increasing the length of A&R wire from installation vessel, and the second step is to pull-in the pull-head by decreasing the length of pull-in wire from platform.

The geometrical relationship in lowering step is shown in Figure 4. Assuming the initial position of pull-head before transfer process is at (x_0, y_0), the increasing length of A&R wire ΔL will change the pull-head position to (x_1, y_1), S_0 is the suspended segment length of the SCR at the initial position, S_1 is the suspended segment length of the SCR after lowering, Δx is the horizontal position's change of TDP, Δx_1

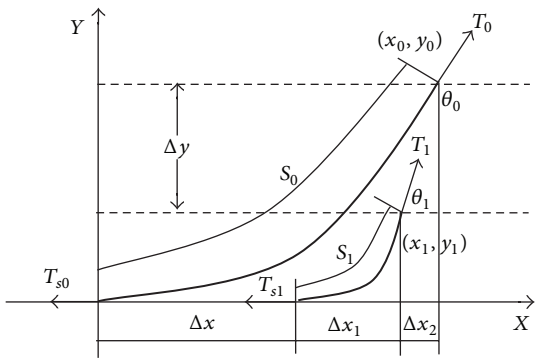

Figure 4: Geometrical relationship for lowering step.

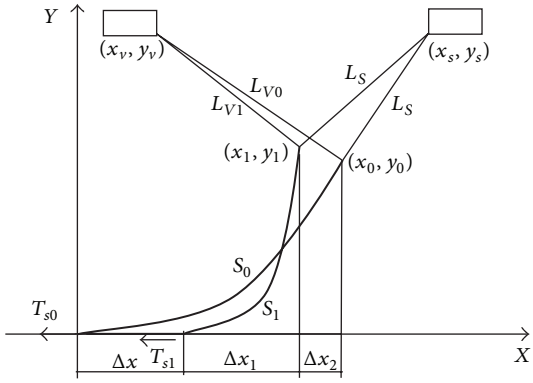

Figure 5: Geometrical relationship for pull-in step.

is the horizontal length of S_1, Δx_2 is the horizontal position change of pull-head, and Δy is the vertical position change of pull-head. The following relations can be obtained:

$$x_0 = \Delta x + \Delta x_1 + \Delta x_2 \tag{3}$$

$$s_0 = \Delta x + s_1. \tag{4}$$

Based on (1)–(4), the pull-head control model for the lowering step can be obtained:

$$\begin{aligned} x_1 = {} & y_0\sqrt{1+2A} - y_1\sqrt{1+2B} \\ & + y_1 B \ln\left[\frac{1}{B} + 1 + \sqrt{\left(\frac{1}{B}+1\right)^2 - 1}\right] \\ & + \Delta L\cos\theta_1, \end{aligned} \tag{5}$$

where $A = \cos\theta_0/(1-\cos\theta_0)$, $B = (1-\cos\theta_1)/\cos\theta_1$.

The geometrical relationship in pull-in step is shown in Figure 5. Assuming the initial position of the installation vessel is at (x_s, y_s), with the initial position of platform being at (x_v, y_v), while the initial position of pull-head is at (x_0, y_0), the increasing length of pull-in wire ΔL will change the pull-head position to (x_1, y_1). S_0 is the suspended segment length of the SCR at initial position, and S_1 is the suspended segment length of the SCR after pull-in, whereas Δx is the horizontal position's change of TDP, Δx_1 is horizontal length of S_1, and

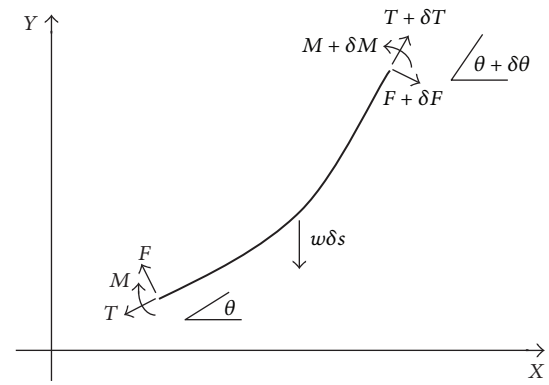

Figure 6: Forces on a large deformation beam segment δs.

Δx_2 is horizontal position's change of pull-head. Therefore, the following equations can be obtained:

$$\begin{aligned} L_S &= \sqrt{(x_S - x_0)^2 + (y_S - y_0)^2} \\ &= \sqrt{(x_S - x_1)^2 + (y_S - y_1)^2} \end{aligned} \tag{6}$$

$$\begin{aligned} \Delta L = {} & \sqrt{(x_v - x_0)^2 + (y_v - y_0)^2} \\ & - \sqrt{(x_v - x_1)^2 + (y_v - y_1)^2} \end{aligned} \tag{7}$$

$$x_0 = \Delta x + \Delta x_1 + \Delta x_2. \tag{8}$$

By combining (1), (2), and (6) in (8), the pull-head control model for the pull-in step can be obtained:

$$\begin{aligned} x_1 = {} & y_0\sqrt{1+2A} - y_1\sqrt{1+2B} \\ & + y_1 B \ln\left[\frac{1}{B} + 1 + \sqrt{\left(\frac{1}{B}+1\right)^2 - 1}\right]. \end{aligned} \tag{9}$$

2.2. SCR Part. An infinitesimal element with length ds based on the nonlinear large deformation beam theory is presented in Figure 6. The force equilibrium equation normal to the segment's axial direction is established by (10), and the force equilibrium equation in the segment's axial direction is established by (11). Consider

$$\delta F - T\delta\theta + w\delta s\cos\theta = 0 \tag{10}$$

$$\delta T = w\delta s\sin\theta, \tag{11}$$

where F is shear force ($F = dM/ds$), T is axial tension, and M is bending moment. Then, (10) can be written as follows:

$$\frac{d^2M}{ds^2} - T\frac{d\theta}{ds} + w\cos\theta = 0. \tag{12}$$

According to large deformation beam theory, the curvature $1/R = M/\mathrm{EI} = d\theta/ds$, where EI is the flexural rigidity. Therefore, (12) can be written in the following form:

$$\frac{d^2}{ds^2}\left(\mathrm{EI}\frac{d\theta}{ds}\right) - T\frac{d\theta}{ds} + w\cos\theta = 0. \tag{13}$$

By simplifying (11) and (13), the mechanical model for large deformation beam can be obtained as follows:

$$\mathrm{EI}\frac{d^3\theta}{ds^3} - T\frac{d\theta}{ds} + w\cos\theta = 0 \tag{14}$$

$$\frac{dT}{ds} = w\sin\theta. \tag{15}$$

The boundary condition at top point of riser is $d\theta_T/d\varepsilon = 0$, and the boundary conditions at TDP are $\theta_D = \theta^*, d\theta_D/d\varepsilon = \sin\theta^*$, and $T(\varepsilon) = F_T\cos\omega_T\cos\theta^*$, where F_T is the lifting load at the top of riser, ω_0 is the angel between lifting load and the x-axis, θ^* is the angel between riser and the x-axis at TDP.

Equation (14) is a third-order nonlinear differential equation with an unknown variable θ. It can be solved using numerical method such as the finite element method [17] or the finite difference method [18]. However, we provide the analytical solution by HAM in this paper.

3. HAM Solution for SCR Installation Model

3.1. Basic Idea of HAM. Perturbation technique has been widely used for nonlinear problem [19] which is dependent on small physical parameters. Liao [20] proposed a general analytical method known as HAM for nonlinear problems by using the basic ideas of the homotopy in topology. HAM provides us with great freedom to select proper base functions for approximate solutions of nonlinear problems and a simple way to get enough accurate analytical approximations.

For the nonlinear differential equations with general form:

$$A[u(x)] = 0 \quad x \in R^n. \tag{16}$$

A is the nonlinear operator for all equations, $u(x)$ is an unknown solution for all equations, and x is the independent variables. Based on the basic concept of HAM, the embedded parameter $p \in [0,1]$ and the initial guess of the exact solution $u_0(x)$ are introduced. The homotopy which is the so-called zero-order deformation equation can be constructed as follows:

$$\begin{aligned}&(1-p)L[\phi(x;p) - u_0(x)]\\ &\quad = p\hbar H(x)A[\phi(x;p)] \quad p \in [0,1],\end{aligned} \tag{17}$$

where $\hbar$ is a nonzero auxiliary parameter, $H(x)$ is a nonzero auxiliary function, L is an auxiliary linear operator that satisfies the property $L[0] = 0$, and $\phi(x;p)$ is an unknown function. It is obvious that, when $p = 0$ and $p = 1$, the following relations hold, respectively:

$$\phi(x;0) = u_0(x), \qquad \phi(x;1) = u(x). \tag{18}$$

Thus, as p increases from 0 to 1, the solution $\phi(x;p)$ varies from the initial guess $u_0(x)$ to the accurate solution $u(x)$. Expand $\phi(x;p)$ by Taylor's theorem in a power series of p:

$$\phi(x;p) = u_0(x) + \sum_{k=1}^{+\infty} u_k(x)\,p^k, \tag{19}$$

where $u_k(x) = (1/k!)(\partial^k\phi(x;p)/\partial p^k)|_{p=0}$.

Assuming that L, $u_0(x)$, $\hbar$, and $H(x)$ are properly chosen; the power series (19) converges at $p = 1$, and the solution series can be obtained as follows:

$$u(x) = u_0(x) + \sum_{k=1}^{+\infty} u_k(x). \tag{20}$$

Differentiating the zero-order deformation equation (17) m times with respect to p, dividing by $m!$, and setting $p = 0$, mth-order deformation equation can be obtained:

$$L[u_k(x) - \chi_k u_{k-1}(x)] = \hbar H(x) R_k(x), \tag{21}$$

where

$$\begin{aligned}\chi_k &= \begin{cases}0, & k \leqslant 1\\ 1, & k > 1,\end{cases}\\ R_k(x) &= \frac{1}{(k-1)!}\left.\frac{\partial^{k-1}A[\phi(x;p)]}{\partial p^{k-1}}\right|_{p=0}.\end{aligned} \tag{22}$$

3.2. Solution of the Mechanical Model for SCR Part by HAM. A dimensionless parameter $\varepsilon = s/l$ is introduced to (14) and (15), and HAM is used to obtain the analytical approximation of this mechanical model.

Assuming that $\varphi^\theta(\varepsilon,q)$ is the homotopy which is connected to the original equation, solution $\theta(\varepsilon)$, and the initial guess solution $\theta_0(\varepsilon)$, $\varphi^T(\varepsilon,q)$ is the homotopy which is connected to the original equation solution $T(\varepsilon)$ and the initial guess solution $T_0(\varepsilon)$. The embedded parameter $q \in [0,1]$, the nonzero auxiliary parameters $\hbar_\theta$ and $\hbar_T$, the auxiliary linear operators L_θ and L_T, and the nonzero auxiliary functions $H_\theta(\varepsilon)$ and $H_T(\varepsilon)$ are introduced. The nonlinear operators for (14) and (15) are

$$\begin{aligned}&N_\theta\left[\varphi^\theta(\varepsilon,q), \varphi^T(\varepsilon,q)\right]\\ &\quad = \frac{\partial^3\varphi^\theta(\varepsilon,q)}{\partial\varepsilon^3} - \frac{l^2}{\mathrm{EI}}\varphi^T(\varepsilon,q)\frac{\partial\varphi^\theta(\varepsilon,q)}{\partial\varepsilon}\\ &\qquad + \frac{wl^3}{\mathrm{EI}}\cos\left[\varphi^\theta(\varepsilon,q)\right]\\ &N_T\left[\varphi^\theta(\varepsilon,q), \varphi^T(\varepsilon,q)\right]\\ &\quad = \frac{\partial\varphi^T(\varepsilon,q)}{\partial\varepsilon} - lw\sin\left[\varphi^\theta(\varepsilon,q)\right].\end{aligned} \tag{23}$$

Thus, zero-order deformation equations can be obtained as follows:

$$\begin{aligned}&(1-q)L_\theta\left[\varphi^\theta(\varepsilon,q) - \theta_0(\varepsilon)\right]\\ &\quad = \hbar_\theta H_\theta(\varepsilon) q N_\theta\left[\varphi^\theta(\varepsilon,q), \varphi^T(\varepsilon,q)\right]\\ &(1-q)L_T\left[\varphi^T(\varepsilon,q) - T_0(\varepsilon)\right]\\ &\quad = \hbar_T H_T(\varepsilon) q N_T\left[\varphi^\theta(\varepsilon,q), \varphi^T(\varepsilon,q)\right]\end{aligned} \tag{24}$$

which satisfies the initial conditions $\varphi^{\theta}(\varepsilon,0) = \theta_0(\varepsilon)$ and $\varphi^{T}(\varepsilon,0) = T_0(\varepsilon)$.

Applying (20) to this case, we can write

$$\begin{aligned}\theta(\varepsilon) &= \varphi^{\theta}(\varepsilon,1) = \varphi^{\theta}(\varepsilon,0) + \sum_{m=1}^{+\infty}\frac{1}{m!}\frac{\partial^m}{\partial q^m}\varphi^{\theta}(\varepsilon,q)\Big|_{q=0} \\ &= \theta_0(\varepsilon) + \sum_{m=1}^{+\infty}\theta_m(\varepsilon) \\ T(\varepsilon) &= \varphi^{T}(\varepsilon,1) = \varphi^{T}(\varepsilon,0) + \sum_{m=1}^{+\infty}\frac{1}{m!}\frac{\partial^m}{\partial q^m}\varphi^{T}(\varepsilon,q)\Big|_{q=0} \\ &= T_0(\varepsilon) + \sum_{m=1}^{+\infty}T_m(\varepsilon),\end{aligned} \tag{25}$$

where $\theta_m(\varepsilon) = (1/m!)(\partial^m/\partial q^m)\varphi^{\theta}(\varepsilon,q)|_{q=0}$ and $T_m(\varepsilon) = (1/m!)(\partial^m/\partial q^m)\varphi^{T}(\varepsilon,q)|_{q=0}$.

The mth-order deformation equations (21) for this particular case are

$$\begin{aligned}&L_{\theta}\left[\theta_m(\varepsilon) - \chi_m\theta_{m-1}(\varepsilon)\right] \\ &\quad = \hbar_{\theta}H_{\theta}(\varepsilon)R_m^{\theta}\left[\theta_{m-1}(\varepsilon), T_{m-1}(\varepsilon)\right] \\ &L_{T}\left[T_m(\varepsilon) - \chi_m T_{m-1}(\varepsilon)\right] \\ &\quad = \hbar_{T}H_{T}(\varepsilon)R_m^{T}\left[\theta_{m-1}(\varepsilon), T_{m-1}(\varepsilon)\right],\end{aligned} \tag{26}$$

where

$$\chi_k = \begin{cases}0, & k \leqslant 1 \\ 1, & k > 1,\end{cases}$$

$$\begin{aligned}&R_m^{\theta}\left[\theta_{m-1}(\varepsilon), T_{m-1}(\varepsilon)\right] \\ &\quad = \theta'''_{m-1}(\varepsilon) - \frac{l^2}{\mathrm{EI}}\sum_{k=0}^{m-1}T_k(\varepsilon)\theta'_{m-1-k}(\varepsilon) \\ &\qquad + \frac{wl^3}{\mathrm{EI}(m-1)!}\frac{\partial^{m-1}}{\partial q^{m-1}}\cos\left[\varphi^{\theta}(\varepsilon,q)\right]\Big|_{q=0}, \\ &R_m^{T}\left[\theta_{m-1}(\varepsilon), T_{m-1}(\varepsilon)\right] \\ &\quad = T'_{m-1}(\varepsilon) - \frac{lw}{(m-1)!}\frac{\partial^{m-1}}{\partial q^{m-1}}\sin\left[\varphi^{\theta}(\varepsilon,q)\right]\Big|_{q=0}.\end{aligned} \tag{27}$$

We select the nonzero auxiliary function as

$$H_{\theta}(\varepsilon) = \frac{s^2}{\mathrm{EIT}}, \qquad H_T(\varepsilon) = \frac{1}{\mathrm{EIT}}. \tag{28}$$

Referring to the catenary equation, we select the initial guess solution $\theta_0(\varepsilon)$ and $T_0(\varepsilon)$ as

$$\theta_0(\varepsilon) = \arctan\left(\frac{awl\varepsilon^k}{G}\right), \qquad T_0(\varepsilon) = \sqrt{(lw\varepsilon)^2 + G^2}, \tag{29}$$

where $G = F_0\cos\omega_0$ and a and k are adjustment parameters which is related to the length of riser l. Through dimensional analysis, the following relationship can be obtained:

$$\frac{l}{l_0} = \left(\frac{\mathrm{EI}w_0}{\mathrm{EI}_0 w}\right)^{1/3}. \tag{30}$$

If we select the length of riser l_0 under the condition $\mathrm{EI}_0 = 50$ and $w_0 = 350.59$, the adjustment parameters a and k can be expressed with respect to l_0:

$$a = \begin{cases}1.02755 - 1.84502e^{-l_0/1.43616} & l_0 \leq 6 \\ 0.947 + 0.009l_0 & l_0 \leq 10 \\ 1.035 & l_0 \leq 14 \\ 1.08931 - 0.00385l_0 & l_0 \leq 23 \\ 0.98683 + 688.37803e^{-l_0/2.11687} & l_0 \leq 26 \\ 0.96059 + 0.00113l_0 & l_0 \leq 40 \\ 1 & l_0 > 40\end{cases}$$

$$k = \begin{cases}0.00541e^{l_0/0.48212} + 1.35738 & l_0 \leq 2 \\ 1.28217e^{-l_0/2.36014} - 0.00781l_0 + 1.19157 & l_0 \leq 25 \\ 1 & l_0 > 25.\end{cases} \tag{31}$$

Considering the boundary conditions at TDP ($\varepsilon = 0$) and top point of riser ($\varepsilon = 1$) in mechanical model for part I, the following boundary conditions can be obtained:

$$\begin{aligned}&\varepsilon = 0\text{: } \theta(\varepsilon) = 0, \quad \frac{d\theta(\varepsilon)}{d\varepsilon} = 0, \quad T(\varepsilon) = F_0\cos\omega_0 \\ &\qquad \varepsilon = 1\text{: } \frac{d\theta(\varepsilon)}{d\varepsilon} = 0.\end{aligned} \tag{32}$$

When the nonzero auxiliary parameters are selected as $\hbar_{\theta} = 0.1$ and $\hbar_T = 1$, the analytical approximate solution of $\theta(\varepsilon)$ and $T(\varepsilon)$ can be written as

$$\begin{aligned}\theta(\varepsilon) &= \arctan\left(\frac{awl_0\varepsilon^k}{G}\right) + \frac{\hbar_{\theta}\varepsilon^2}{\mathrm{EI}_0 T} \\ &\quad \times \left\{\frac{C}{D} - \frac{3C}{kD} - \frac{8a^2\varepsilon^{2k}l_0^2w_0^2C}{G^2D^2} + \frac{2C}{k^2D}\right. \\ &\quad + \frac{6a^2s^{3k}l_0^2w_0^2C}{\varepsilon^k kG^2D^2} + \frac{8a^4s^{5k}l_0^4w_0^4C}{\varepsilon^k G^4D^3} \\ &\quad \left. + \frac{l_0^3\left[(l_0w_0s)^2 + G^2\right]^{0.5}\varepsilon^2C}{\mathrm{EI}_0k^2l_0D} + \frac{l_0^3w_0}{\mathrm{EI}_0D^{0.5}}\right\} \\ T(\varepsilon) &= \sqrt{(lw\varepsilon)^2 + G^2} + \frac{\hbar_T}{\mathrm{EIT}} \\ &\quad \times \left\{\frac{l^2w^2\varepsilon}{\left[(lw\varepsilon)^2 + G^2\right]^{0.5}} - lw\sin\left[\arctan\left(\frac{wl\varepsilon}{G}\right)\right]\right\},\end{aligned} \tag{33}$$

where $C = a\varepsilon^k k^3 l_0 w_0/\varepsilon^3 G$, $D = 1 + (a^2\varepsilon^{2k}l_0^2w_0^2/G^2)$.

Table 1: Parameters of SCR.

Parameter	Value
Outer diameter (m)	0.3048
Inner diameter (m)	0.2743
Flexural rigidity (N·m^2)	3.1340E07
Weight submerged (N/m)	350.59
Density (kg/m^3)	7850

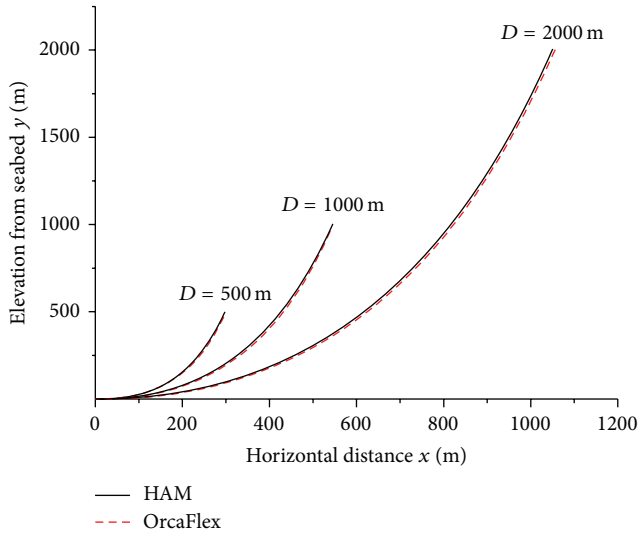

Figure 7: Configuration results comparison between HAM and OrcaFlex in different water depth.

4. Results and Discussion

In order to implement the SCR installation model as described above, a computer program has been developed within the framework of MATLAB language program. The efficiency and accuracy of this model is verified by comparison with the numerical results of OrcaFlex. The parameters of SCR used for verification and analysis are detailed in Table 1.

The overall configuration and axial tension calculated by the proposed method and OrcaFlex are compared as shown in Figures 7 and 8, respectively. In different water depth conditions, the results are well coincided, which prove that the analytical method is accurate and can be used to analyze SCR installation problem. Some critical parameters are summarized in Table 2, where X is horizontal distance from TDP to the top point of riser, Y_{top} is vertical distance from seabed, and T_{max} is maximum axial tension at the top point of riser.

Postlay method is selected for SCR installation parameters analysis. In this method, the offshore platform is on site. When SCR is laid near to the offshore platform by installation vessel, SCR pull-head is firstly connected to the A&R wire and the cable from offshore platform, which is lifted only by the A&R wire. Increase the length of A&R wire to lower pull-head to the maximum depth and then decrease the length of cable from offshore platform until pull-head is finally lifted to the hang-off position. Note that the dynamic positioning (DP) system always maintains the installation vessel and offshore platform position in the original place during SCR installation.

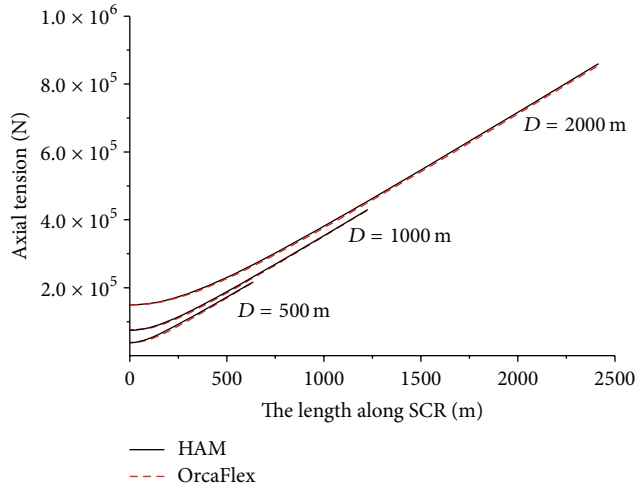

Figure 8: Axial tension results comparison between HAM and OrcaFlex in different water depth.

The safety of SCR during installation is affected by many factors. The most important one is that the variation of SCR maximum stress caused by the change of installation shape should be within the allowable stress. In order to investigate the influence of the initial installation angle, the maximum lower depth of pull-head, water depth, and the distance between installation vessel and offshore platform, the parameters shown in Table 1 are used for SCR, with following hypotheses.

(1) Assume that the initial installation angle is θ_I, the maximum lower depth of pull-head is D_L, water depth is D, and the distance between installation vessel and offshore platform is D_V.

(2) Assume that the horizontal position of pull-head is X_{ph}, which has zero value at the position of the installation vessel and has maximum value at the position of the offshore platform.

(3) Assume that the vertical position of pull-head is Y_{ph}, which has zero value at sea level and has maximum value at D_L.

The maximum stress results under different conditions are summarized in Table 3.

4.1. Influence of θ_I. Usually, deepwater SCR is installed by J-lay vessel, and the installation angle (the angle between the J-lay tower and the vertical direction) will affect the SCR installation shape. Under the conditions that D_L is 30 m, D_V is 35 m, D is 1000 m, and θ_I is 8°, 10° and 12°, respectively, the maximum stresses of SCR during installation are shown in Figure 9. It clearly shows that, with the small rise of θ_I, the maximum stresses on SCR increase rapidly. It can be observed that the J-lay method is more suitable for deepwater SCR installation than S-lay method, since it can control the θ_I nearly to zero.

Table 2: Critical results.

Item	$D = 500$ m			$D = 1000$ m			$D = 2000$ m		
	X (m)	Y_{top} (m)	T_{max} (N)	X (m)	Y_{top} (m)	T_{max} (N)	X (m)	Y_{top} (m)	T_{max} (N)
HAM	297.97	499.41	217071	545.43	1004.09	429937	1050.67	2006.54	859997
OrcaFlex	299.89	499.91	214430	546.57	1002.77	428228	1056.20	2003.68	853240
Difference	0.64%	−0.1%	−1.23%	0.21%	−0.13%	−0.4%	0.53%	−0.14%	−0.79%

Table 3: Maximum stress results.

θ_I (°)	D_L (m)	D (m)	D_V (m)	σ_{max} (MPa)
8	30	1000	35	169.37
10	30	1000	35	215.15
12	30	1000	35	273.91
10	33	1000	35	218.09
10	36	1000	35	221.10
10	35	1000	35	219.98
10	35	1500	35	135.79
10	35	2000	35	100.23
10	35	1000	30	217.84
10	35	1000	40	222.21

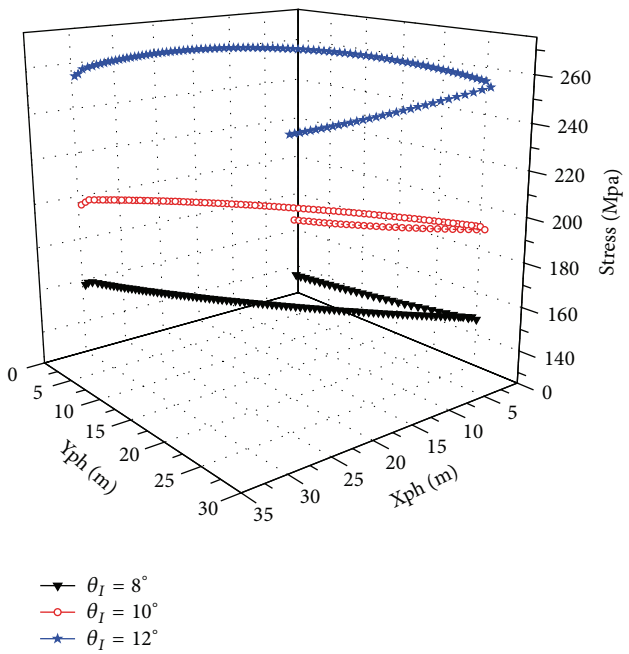

Figure 9: Maximum stresses in different θ_I.

4.2. Influence of D_L. Under the condition that θ_I is 10°, D_V is 35 m, D is 1000 m, and D_L is 30 m, 33 m, and 36 m, respectively, the maximum stresses of SCR during installation are shown in Figure 10. The calculated results show that, with the rise of D_L, the maximum stresses on SCR increase accordingly. It is necessary to control D_L at its minimum value in order to avoid the interference of auxiliary installation equipment to keep SCR under safe condition.

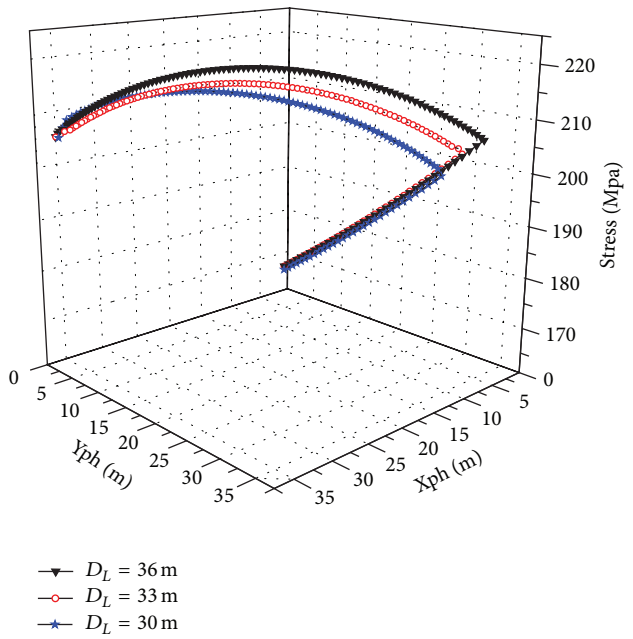

Figure 10: Maximum stresses in different D_L.

4.3. Influence of D. Under the condition that θ_I is 10°, D_V is 35 m, D_L is 35 m, and D is 1000 m, 1500 m, and 2000 m, respectively, the maximum stresses on SCR during installation are shown in Figure 11. The calculated results show that, with the decrease of D, the maximum stresses on SCR increase rapidly. It is necessary to pay more attention to the control of installation path in shallow water. This is because the SCR length increases as water depth increases, and the relative change in installation shape is greater in shallow water than in deep water.

4.4. Influence of D_V. Under the condition that θ_I is 10°, D is 1000 m, D_L is 35 m, and D_V is 30 m, 35 m, and 40 m, respectively, the maximum stresses on SCR during installation are shown in Figure 12. The calculated results show that, with the rise of D_V, the maximum stresses on SCR increase accordingly. It can be inferred that, for the safety of installation vessel and offshore platform, smaller values of D_V are preferred for SCR installation.

5. Conclusion

A simple model for analyzing the static behavior of the deep-water SCR during installation is proposed, while the nonlinear large deformation beam theory is applied and HAM

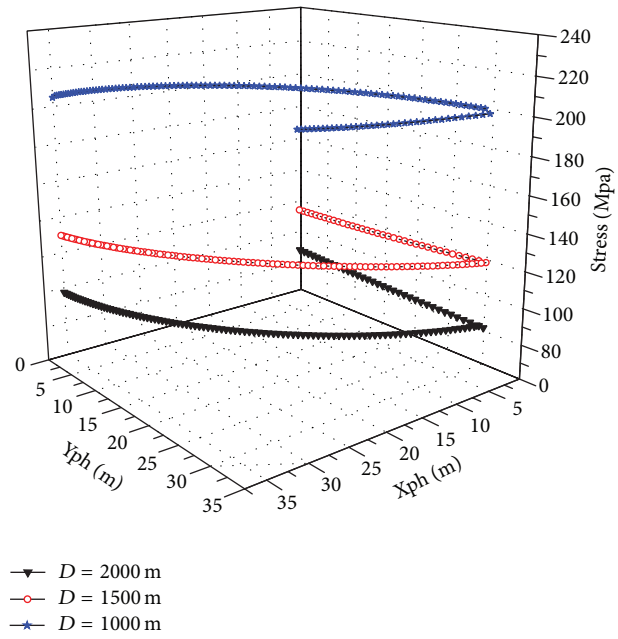

Figure 11: Maximum stresses in different D.

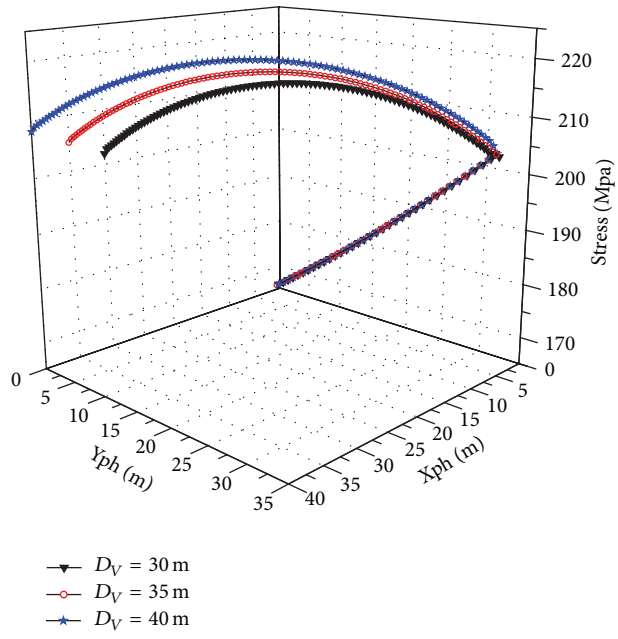

Figure 12: Maximum stresses in different D_V.

is used to obtain an analytical approximate solution for this model. This model has the main advantage of time-saving and its practicality. In comparison with the results calculated using the software OrcaFlex, a positive agreement is obtained, which demonstrates that the analytical approximate solution is reliable.

The presented model is applied to analyze the influence of different parameters. Some valuable conclusions can be drawn as follows.

(1) Larger initial installation angle causes higher maximum stress during SCR installation, and the J-lay tower is preferred to be placed in an almost vertical position during SCR installation in order to reduce the initial installation angle.

(2) The maximum stress during SCR installation increases with the lower depth of pull-head. The pull-head should be controlled at the minimum lower depth to keep the safety of SCR during installation.

(3) As water becomes deeper, the maximum stress during SCR installation becomes smaller, which is beneficial to the safety of SCR. However, the increasing axial tension induced by its self-weight brings higher requirements on the capacity of the installation vessel.

(4) A longer distance between the installation vessel and the offshore platform can cause a little increase in the maximum stress during SCR installation. To avoid the interference between the installation vessel and the offshore platform, a smaller distance between them is preferred for SCR installation.

This paper reports reasonable approach to the deepwater SCR installation analysis. However, as some assumptions are made for simplifying the investigation, further work needs to be carried out to integrate these assumptions, such as the effect of pipe-soil interaction.

Conflict of Interests

The authors declare that there is no conflict of interests regarding the publication of this paper.

Acknowledgments

This paper is financially supported by the National Natural Science Foundation of China (Grant no. 51349002), the China National Science and Technology Major Projects on Pipe Laying and Lifting Vessel (Grant no. 2011ZX05027-002), and the Higher Education Specialized Research Fund for the Doctoral Program (Grant no. 20130007120009). Sincerely, the authors' thanks also go to colleagues in the COOEC Ltd. and Offshore Oil/Gas Research Centre of CUP, who are involved in this wide range of researches. The authors also highly appreciate the reviewers and the editors' careful checking and valuable comments on this paper.

References

[1] F. Kopp and D. W. Barry, "Design and installation of auger pipelines," in *Proceedings of the 1994 Offshore Technology Conference*, Houston, Tex, USA, 1994.

[2] G. Chaudhury, J. Kennefick, and J. R. McDermott, "Design, testing, and installation of steel catenary risers," in *Proceedings of the 31st Annual Offshore Technology Conference (OCT '99)*, Houston, Tex, USA, May 2000.

[3] J. van der Graaf, D. Wolbers, and P. Boerkamp, "Field experience with the construction of large diameter steel catenary risers in deep water," in *Proceedings of the Offshore Technology Conference*, Houston, Tex, USA, May 2005.

[4] X. Wang and X. Zhou, "Installation method evaluation of export SCRs," in *Proceedings of the 2001 Offshore Technology Conference*, Houston, Tex, USA, May 2001.

[5] Y. Bai and Q. Bai, *Subsea Pipelines and Risers*, Elsevier, Amsterdam, The Netherlands, 2005.

[6] Y. Nishi, "Static analysis of axially moving cables applied for mining nodules on the deep sea floor," *Applied Ocean Research*, vol. 34, pp. 45–51, 2012.

[7] P. S. Charles, *Fundamentals of Marine Riser Mechanical: Basic Principles and Simplified Analyses*, PennWell, Tulsa, Okla, USA, 2007.

[8] X. G. Zeng, M. L. Duan, and J. H. Chen, "Resarch on several mathematical models of offshore pipe lifting or lowering by one point," *The Ocean Engineering*, vol. 31, no. 1, pp. 32–37, 2013.

[9] D. A. Dixon and D. R. Rultledge, "Stiffened catenary calculation in pipeline laying problem," *Journal of Engineering for Industry*, vol. 90, no. 1, pp. 153–160, 1968.

[10] F. Guarracino and V. Mallardo, "A refined analytical analysis of submerged pipelines in seabed laying," *Applied Ocean Research*, vol. 21, no. 6, pp. 281–293, 1999.

[11] Y. J. Dai, J. Z. Song, and G. Feng, "A study on abandonment and recovery operation of submarine pipelines," *Ocean Engineering*, vol. 18, no. 3, pp. 75–78, 2000 (Chinese).

[12] Z. J. Xing, T. C. Liu, and X. H. Zeng, "Nonlinear analysis of submarine pipelines during single point lifting," *Ocean Engineering*, vol. 20, no. 3, pp. 29–33, 2002 (Chinese).

[13] S. Lenci and M. Callegari, "Simple analytical models for the J-lay problem," *Acta Mechanica*, vol. 178, no. 1-2, pp. 23–39, 2005.

[14] J. García-Palacios, A. Samartin, and V. Negro, "A nonlinear analysis of laying a floating pipeline on the seabed," *Engineering Structures*, vol. 31, no. 5, pp. 1120–1131, 2009.

[15] T. K. Datta, "Abandonment and recovery solution of submarine pipelines," *Applied Ocean Research*, vol. 4, no. 4, pp. 247–252, 1982.

[16] C. P. Sparks, *Fundamentals of Marine Riser Mechanics: Basic Principles and Simplified Analyses*, Penn Well Corporation, Tulsa, Okla, USA, 2007.

[17] I. K. Chatjigeorgiou, "A finite differences formulation for the linear and nonlinear dynamics of 2D catenary risers," *Ocean Engineering*, vol. 35, no. 7, pp. 616–636, 2008.

[18] H. Park and D. Jung, "A finite element method for dynamic analysis of long slender marine structures under combined parametric and forcing excitations," *Ocean Engineering*, vol. 29, no. 11, pp. 1313–1325, 2002.

[19] A. H. Nayfeh, *Perturbation Methods*, Cambridge University Press, London, UK, 1973.

[20] J. S. Liao, *The proposed homotopy analysis technique for the solution of nonlinear problems [Ph.D. thesis]*, Shanghai Jiao Tong University, 1992.